

Memory-augmented Adversarial Autoencoders for Multivariate Time-series Anomaly Detection with Deep Reconstruction and Prediction

Qinfeng Xiao, Shikuan Shao, Jing Wang

Beijing Jiaotong University
qfxiao, skshao, wj@bjtu.edu.cn

Abstract

Detecting anomalies for multivariate time-series without manual supervision continues a challenging problem due to the increased scale of dimensions and complexity of today’s IT monitoring systems. Recent progress of unsupervised time-series anomaly detection mainly use deep autoencoders to solve this problem, i.e. training on normal samples and producing significant reconstruction error on abnormal inputs. However, in practice, autoencoders can reconstruct anomalies so well, due to powerful capabilities of neural networks. Besides, these approaches can be ineffective for identifying non-point anomalies, e.g. contextual anomalies and collective anomalies, since they solely utilize a point-wise reconstruction objective. To tackle the above issues, we propose MemAAE (*Memory-augmented Adversarial Autoencoders with Deep Reconstruction and Prediction*), a novel unsupervised anomaly detection method for time-series. By jointly training two complementary proxy tasks, reconstruction and prediction, with a shared network architecture, we show that detecting anomalies via multiple tasks obtains superior performance rather than single-task training. Additionally, a compressive memory module is introduced to preserve normal patterns, avoiding unexpected generalization on abnormal inputs. Through extensive experiments, MemAAE achieves an overall F1 score of 0.90 on four public datasets, significantly outperforming the best baseline by 0.02.

Introduction

Detecting anomalies for time-series is critical for various fields, e.g. web service maintenance (Xu et al. 2018), industry device monitoring (Su et al. 2019; Tian et al. 2019), cyber intrusion detection (Li et al. 2019) and anomalous rhythm detection (Zhou et al. 2019). Since anomalies appeared in time-series indicate failures of machines or symptoms of human bodies, automatic anomaly detection is of significant importance for many practical applications. Traditional strategies detect anomalies via supervised classifiers (Liu et al. 2015), namely considering the anomaly detection problem as a binary classification task. However, supervised anomaly detection faces exact challenges including imbalanced classes, heavy labeling cost and presence of unseen anomalous patterns, which limit the use of them in practical situations. Recently, deep autoencoders have drawn extensive attention for time-series anomaly detection (Xu et al. 2018; Su et al. 2019; Li et al. 2019; Audibert et al.

2020). By training variational autoencoders (VAE) or Generative Adversarial Networks (GAN) on normal data, the model is expected to produce higher reconstruction errors for anomalies. However, the problem of unsupervised multivariate time-series anomaly detection is still challenging due to the following questions:

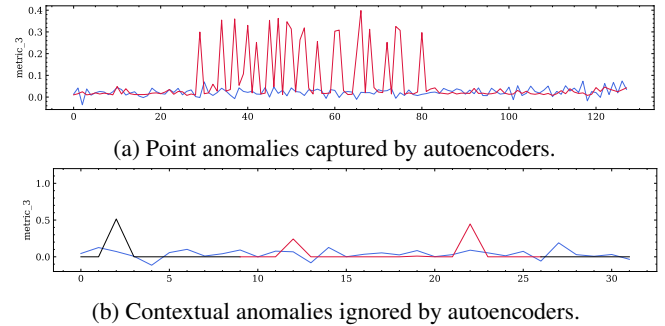


Figure 1: Examples of anomaly detection using conventional reconstruction-based method, where black lines, red lines and blue lines indicate normal observations, anomalies and reconstructions respectively.

1) *Complexity of multivariate time-series.* Today’s developing of IT monitoring systems and increasing dimensions of time-series render the difficulty of anomaly detection. As internal complexities of data grow exponentially, autoencoders’ capability of modeling data distribution has seriously overstretched. To this end, integration of modern techniques, e.g. GAN (Goodfellow et al. 2014), are desired.

2) *Heterogeneous types of anomalies.* As described in previous researches (Chandola, Banerjee, and Kumar 2009; Chalapathy and Chawla 2019), anomalies are categorized into different classes, e.g. point anomaly, contextual anomaly and collective anomaly. Point anomalies can be effectively detected by reconstruction-based models (showing in Figure 1a), since they use a point-wise reconstruction error. However, contextual anomalies and collective anomalies can be hard to captured by them because they violate the normal patterns only in the “context” rather than obviously deviating the normal value range (anomalies in Figure 1b are hard to be identified by reconstruction error).

3) *Unexpected generalization on abnormal inputs.* The

autoencoder can reconstruct anomalous samples so well because of the powerful generalization capabilities of neural networks. Many reasons can contribute to the phenomenon, such as an over-fitting autoencoder, structural similarities between anomalous and normal samples, leading an unclear boundary between anomalies and normalities. Besides, unlabeled anomalies in the training data (termed Anomaly Contamination) can significantly aggravate this issue since autoencoders are trained to minimize reconstruction error for them as well.

To address the above challenges, we propose MemAAE (*Memory-augmented Adversarial Autoencoders with Deep Reconstruction and Prediction*), a novel unsupervised anomaly detection model for multivariate time-series. Specifically, we improve conventional autoencoders with three dedicated modules to solve the issues respectively. The first is the use of adversarial training (Goodfellow et al. 2014). Unlike relevant researches that directly use the GAN model (Zenati et al. 2018; Li et al. 2019), we use adversarial autoencoders (AAE) (Makhzani et al. 2015) combined with the point-wise reconstruction objective instead. The second is an additional prediction branch. Compared with reconstruction, predicting near future values can be sensitive for contextual and collective anomalies since the prediction task incorporates temporal information over instances, which is ignored by the reconstruction task. The third is a memory mechanism. Instead of allowing the latent variable spreads the whole space or just applying some sparse regularization (such as standard Gaussian distribution), we rebuild the latent vector by the linear combination of normal patterns from the memory module. The memory module can be viewed as a dictionary that stores the basis of the normal manifold. Then the encoder plays the role of determining weights of memory slots (vectors in the memory module). In this way, the burden of modelling the normal patterns is designated to the memory module.

In summary, this paper makes the following three major contributions:

- We propose a novel unsupervised framework, MemAAE, for multivariate time-series anomaly detection. It adopts a simple and effective autoencoder architecture, incorporating with an adversarial training mechanism.
- We extend MemAAE with a memory module, which explicitly models the normality manifold. By enforcing reconstructions are computed by only normal patterns of the memory module, MemAAE can largely avoid unexpected generalization for anomalous samples.
- We augment MemAAE with a prediction module, a complementary training task for the reconstruction. Forecasting future can be more sensitive for contextual and collective anomalies, which finely makes up for the reconstruction task.
- Through extensive experiments, we show that MemAAE achieves an **overall F1 score of 0.90** on four real-world datasets, showing the benefits of utilizing the memory module and the prediction task. Besides, further experiments including sensitivity test of hyperparameters and

ablation study demonstrate effectiveness and robustness of our proposed method.

Related Works

Time-series anomaly detection is an active research topic that has been largely studied (Aggarwal 2016; Chandola, Banerjee, and Kumar 2009; Chalapathy and Chawla 2019; Gupta et al. 2013; Braei and Wagner 2020). Traditional approaches of anomaly detection mainly focus on utilizing prior assumptions on normal patterns which can be categorized into distance-based (Ramaswamy, Rastogi, and Shim 2000; Chaovalitwongse, Fan, and Sachdeo 2007), density-based (Breunig et al. 2000; Ma and Perkins 2003), isolation-based (Liu, Ting, and Zhou 2008) and statistic-based (Siffer et al. 2017; Li et al. 2020) methods.

Prediction-based Time-series Anomaly Detection. Recently, deep learning empowered anomaly detection has draw extensive attention (Pang et al. 2021). A line of works focus on utilizing prediction errors to detect anomalies since they are relatively unpredictable compared with normal points. EGADS (Laptev, Amizadeh, and Flint 2015) is a generic prediction-based anomaly detection framework developed by *Yahoo*. In (Hundman et al. 2018) and (Filonov, Lavrentyev, and Vorontsov 2016), Long-short Term Memory (LSTM) is applied to detect anomalies via prediction errors. However, the performance of prediction-based methods heavily rely on the capability of the prediction model. Since complicated time-series are hard to be accurately predicted, the effectiveness of prediction-based anomaly detection is largely limited.

Reconstruction-based Time-series Anomaly Detection. Another paradigm of anomaly detection uses reconstruction errors to detect anomalies. To achieve this, various autoencoders are used, such as VAE (Xu et al. 2018; Li, Chen, and Pei 2018), Recurrent Neural Network (RNN) based autoencoders (Malhotra et al. 2016; Park, Hoshi, and Kemp 2018; Su et al. 2019; Kieu et al. 2019; Li et al. 2021) and GAN (Goodfellow et al. 2014) based Autoencoders (Li et al. 2019; Audibert et al. 2020). However, reconstruction-based anomaly detection is problematic for two main reasons. Firstly, more powerful the autoencoder is, more risky that anomalies to be well reconstructed during inference phase. Well-reconstructed anomalies can heavily hurt the performance of anomaly detection. Secondly, global anomalies can be effectively captured by reconstruction errors but local contextual anomalies can be insensitive for them.

Multi-task Learning for Anomaly Detection. Multi-task learning (Zhang and Yang 2021) demonstrates the effectiveness of training multiple tasks using a shared network architecture. Existed works considering multi-task learning for anomaly detection include detecting abnormal events in videos (Georgescu et al. 2021; Zhao et al. 2017) and identifying anomalous driving (Sadhu, Misu, and Pompili 2019). However, the application on time-series anomaly detection is largely lagging behind.

Memory Models. In the literatures, memory plays a fundamental role of building deep learning systems for both earlier and recent models, e.g. caching previous states in LSTM and Gated Recurrent Units (GRU) (Hochreiter and Schmidhuber 1997; Chung et al. 2014), and storing history representations in contrastive representation learning (Wu et al. 2018; He et al. 2020). As for anomaly detection, previous works (Gong et al. 2019; Park, Noh, and Ham 2020) have utilized memory to prevent unexpected generalization on anomalous inputs. However, they are not prepared for time-series and can not address all major challenges of time-series anomaly detection mentioned before.

Methodology

Problem Setup

Time-series anomaly detection. Giving a multivariate time series $\mathbf{X} = \{x_1, x_2, \dots, x_N\}$, $x_i \in \mathbb{R}^K$, of N observations and K variables, the goal of **time series anomaly detection** is to learn a scoring function $\phi(\cdot)$ that assigns anomaly scores to each observation such that we have $\phi(x_i) > \phi(x_j)$ if x_i is anomalous and x_j is normal. Detailed description of input format and data preprocessing are listed in the appendix.

Overview

As shown in Figure 2, MemAAE mainly consists of following modules:

- **Autoencoder with adversarial training.** Same as existed time-series anomaly detection works (Audibert et al. 2020; Su et al. 2019), we use the Autoencoder (AE) (Rumelhart, Hinton, and Williams 1985) as our basic model to perform the reconstruction task, where anomalies are expected to obtained higher reconstruction error. However, AE, as well as its variant VAE (Kingma and Welling 2014), uses a “pixel-level” reconstruction error, e.g. ℓ_2 distance of AE and log-likelihood of VAE, to measure the deviation of reconstructed samples w.r.t. input ones. The “pixel-level” reconstruction error can be too strict and results in over-smoothed samples (see Figure 1b). To tackle this issue, we use an additional discriminator to distinguish the true input samples and reconstructed samples (Goodfellow et al. 2014). This technique makes reduced blurriness and enriched details for the reconstruction since the discriminator focus on similarities of the whole distribution.
- **Memory module.** In order to reduce well-reconstructed anomalies, we use a dedicated memory module to preserve the normality manifold. Specifically, the memory module is a dictionary of vectors where each vector is a representative point of the normality manifold. In the reconstruction process, the query, produced by the encoder, is used to draw memory vectors from the memory and the latent vector is inferred by the linear combination of retrieved memory vectors. This ensures reconstructions of the decoder is strictly reconstructed by normal patterns.
- **Prediction module.** To detect contextual and collective anomalies, we design a prediction branch based on the

latent vectors obtained by the memory module that predicts near future values. The reconstruction branch and the prediction branch share the same encoder structure. We assume that anomalies can not be well predicted since they deviate the normal patterns. In the detection phase, the anomaly score is determined by reconstruction error and prediction error together.

Next, we will describe the details of each module in the following sections.

Memory-augmented Adversarial Autoencoder

Encoder and decoder. The autoencoder consists of an encoder and a decoder. The encoder $f_e(\cdot)$ takes the input \mathbf{x} and maps it into a latent vector \mathbf{z} . The decoder $f_d(\cdot)$ maps the latent vector back to the input space to obtain the reconstructed sample $\hat{\mathbf{x}}$. Formally, the process can be defined as:

$$\mathbf{z} = f_e(\mathbf{x}), \quad (1)$$

$$\hat{\mathbf{x}} = f_d(\hat{\mathbf{z}}). \quad (2)$$

For standard autoencoders, we have $\hat{\mathbf{z}} = \mathbf{z}$. In MemAAE, we use \mathbf{z} to retrieve the latent vector $\hat{\mathbf{z}}$ from memory, which will be introduced later. The deviation between the input sample and the reconstruction is measured by the reconstruction error, e.g. ℓ_2 distance:

$$\mathcal{L}_{\text{rec}} = \|\mathbf{x} - \hat{\mathbf{x}}\|_2. \quad (3)$$

The objective of a standard AE is to minimize the reconstruction error \mathcal{L}_{rec} . Autoencoder-based anomaly detection methods use \mathcal{L}_{rec} as the anomaly score while samples of high reconstruction error are considered to be anomalies.

Adversarial training A common issue of the vanilla autoencoder is that MSE loss leads over-smoothed reconstructions. We use adversarial training to tackle this problem. In detail, an additional discriminator $\phi(\cdot)$ is used to distinguish input samples and reconstructions. The objective of adversarial training is:

$$\mathcal{L}_{\text{adv}} = \mathbb{E}_{\mathbf{x} \sim p_{\text{data}}(\mathbf{x})} [\log(\phi(\mathbf{x}))] + \mathbb{E}_{\hat{\mathbf{x}} \sim p_{\text{gen}}(\hat{\mathbf{x}})} [\log(1 - \phi(\hat{\mathbf{x}}))], \quad (4)$$

where p_{data} denotes the ground truth data distribution and p_{gen} denotes the distribution of reconstructed samples. Thus the overall objective of autoencoder training becomes:

$$\mathcal{L}_{\text{full-adv}} = \mathcal{L}_{\text{adv}} + \lambda \cdot \mathcal{L}_{\text{rec}}, \quad (5)$$

where λ is the weight of the reconstruction objective.

Memory module. In order to enable normality manifold preserving, we augment the autoencoder with a dedicated memory module. The latent vector to be feed into the decoder is computed by retrieving items of the memory module and taking linear combination of them. The vector produced by the encoder plays the role to compute the weights over memory slots, which means the burden of modeling normal patterns is allocated to the memory module rather than the encoder. The memory module is shared during the whole training phase.

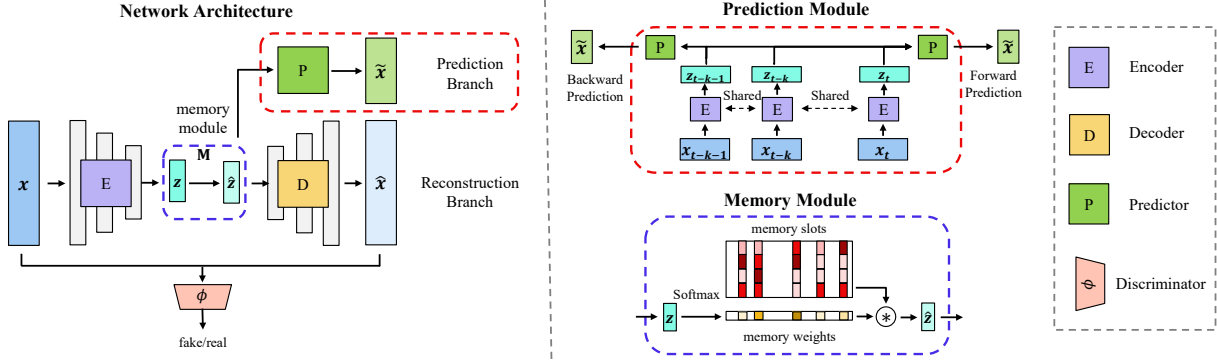


Figure 2: Systematic overview of our proposed model. MemAAE mainly contains three modules: (1) **Autoencoder with adversarial training**. This part is the basic module to perform the reconstruction task. Reconstructed samples are constrained to be as close as input samples under the “pixel level” (by ℓ_2 distance) and “global level” (by adversarial loss) criterions simultaneously. (2) **Memory module**. As the right hand side shows, the memory module is used to model the normality manifold, which consists of a sequence of memory vectors. In the reconstruction phase, the weights of each memory vector is inferred by the output of the encoder. The latent vector to be feed into the decoder is obtained by the linear combination of memory vectors over the weights. (3) **Prediction module**. To detect contextual and collective anomalies, a dedicated prediction branch is incorporated with our model. By aggregating latent vectors over a time window, MemAAE predicts past and future values simultaneously. In the evaluation phase, reconstruction errors and prediction errors are used to detect anomalies.

In detail, the memory module is composed of a matrix $\mathbf{M} = [\mathbf{m}_1, \dots, \mathbf{m}_M] \in \mathbb{R}^{M \times K}$ where M is the memory size and K is the dimension of each memory slot \mathbf{m}_i . Given a query \mathbf{z} , the latent vector $\hat{\mathbf{z}}$ is computed by the linear combination of memory slots:

$$\hat{\mathbf{z}} = \sum_{i=1}^M \mathbf{w}_i \cdot \mathbf{m}_i = \mathbf{w}\mathbf{M}, \quad (6)$$

where \mathbf{w}_i refers to the contribution of the i -th memory slot \mathbf{m}_i and is obtained by the query \mathbf{z} . In practice, the query \mathbf{z} is the vector produced by the encoder, namely $\mathbf{z} = f_e(\mathbf{x})$.

The memory weights \mathbf{w} over memory slots can be obtained by multiple approaches. Gong et al. (2019) computes the weights via an attention manner. For simplicity, we directly assign the normalized query vector as the memory weights. Since the dimension of the query and the memory size are not required to be matched, we first map the query into the \mathbb{R}^M space vis a projection head $\psi(\cdot)$. Then the weights are normalized by `Softmax` function:

$$\mathbf{w} = \text{Softmax}(\psi(\mathbf{z})). \quad (7)$$

In the reconstruction task, the decoder is restricted to use representations acquired from the normality manifold only. To get reliable reconstructions, the memory module is forced to record most representative normal patterns.

Future Forecasting for Anomaly Detection

The above mentioned memory-augmented reconstruction is strong enough to detect point anomalies. However, reconstruction based anomaly detection can be insensitive with contextual and collective anomalies. These anomalies are hard to be captured by reconstruction error because they

deviate normal characteristics only (e.g. seasonality) or depend on previous observations. Thus we propose to leverage future prediction for anomaly detection. Compared with reconstruction, future prediction is more sensitive for local and contextual anomalies since they are hard to be predicted. The details of the future prediction for anomaly detection are introduced in the following.

Structure of prediction branch. The prediction branch $g(\cdot)$ can be implemented by any autoregressive model, such as recurrent neural networks (RNN). In this paper, we use LSTM (Hochreiter and Schmidhuber 1997) to perform the prediction task. The prediction of a sample at time t is computed by aggregating past k latent vectors:

$$\tilde{\mathbf{x}}_t = g(\hat{\mathbf{z}}_{t-k-1}, \dots, \hat{\mathbf{z}}_{t-1}). \quad (8)$$

Weighted decay loss for prediction. To make prediction close to the ground truth, we minimize the ℓ_2 distance between a predicted sample $\tilde{\mathbf{x}}_t$ at time t and its ground truth \mathbf{x}_t :

$$d(\mathbf{x}_t, \tilde{\mathbf{x}}_t) = \|\mathbf{x}_t - \tilde{\mathbf{x}}_t\|_2. \quad (9)$$

Besides, similar with Zhao et al. (2017), we assume predictions for closer time-steps are more important. Thus we reweight the contribution of each prediction according to their temporal distances. The prediction objective can be formulated as a weighted sum of predictions over predicted time-steps:

$$\mathcal{L}_{\text{pred}} = \frac{1}{T^2} \sum_{i=1}^T (T-i) \cdot d(\mathbf{x}_{t+i}, \tilde{\mathbf{x}}_{t+i}), \quad (10)$$

where T is the number of prediction steps.

Bi-directional prediction. Although forecasting future is natural from the perspective of human perception, predicting backwards is also feasible for our model. Besides, leveraging bi-directional prediction for anomaly detection can make full use of data since temporal correlations are naturally bi-directional. Similar with forward prediction, we use an identical predictor $g'(\cdot)$ to perform the backward prediction:

$$\tilde{\mathbf{x}}_t = g'(\hat{\mathbf{z}}_{t+k+1}, \dots, \hat{\mathbf{z}}_{t+1}). \quad (11)$$

Given the time window $\{\mathbf{x}_{t-W+1}, \dots, \mathbf{x}_t\}$, the backward prediction objective is formalized as forecasting T predecessors of the window:

$$\mathcal{L}_{\text{pred-back}} = \frac{1}{T^2} \sum_{i=1}^T (T-i) \cdot d(\mathbf{x}_{t-W-i}, \tilde{\mathbf{x}}_{t-W-i}), \quad (12)$$

where W represents the size of the time window and T indicates the number of prediction steps.

Finally, the full objective is a combination of adversarial loss, reconstruction loss and two prediction losses:

$$\mathcal{L}_{\text{full}} = \mathcal{L}_{\text{adv}} + \lambda \cdot \mathcal{L}_{\text{rec}} + \gamma_1 \cdot \mathcal{L}_{\text{pred}} + \gamma_2 \cdot \mathcal{L}_{\text{pred-back}}, \quad (13)$$

where λ , γ_1 and γ_2 are the weights of reconstruction loss, forward prediction loss and backward prediction loss respectively.

Anomaly Detection

In the detection stage, we calculate anomaly scores for testing samples based on our trained model. As described in the above sections, anomalies are expected to obtain larger reconstruction error and prediction error. Thus we use them to calculate the anomaly score. Formally, the anomaly score $\mathcal{S}(\cdot)$ of a sample \mathbf{x} is defined as :

$$\mathcal{S}(\mathbf{x}) = \lambda \cdot \mathcal{L}_{\text{rec}} + \gamma_1 \cdot \mathcal{L}_{\text{pred}} + \gamma_2 \cdot \mathcal{L}_{\text{pred-back}}, \quad (14)$$

where λ , γ_1 and γ_2 are weights to adjust each term, with same values in Equation 13.

In real-world applications, weather \mathbf{x} is an anomaly can be identified by a pre-defined threshold, which is choosed by the operator. Following recent researches (Xu et al. 2018; Li, Chen, and Pei 2018; Audibert et al. 2020), we focus on anomaly scoring rather than threshold defining.

Experiments

Datasets and Evaluation Metrics

We use four public multivariate time-series datasets to evaluate our model: *Soil Moisture Active Passive (SMAP) satellite, Mars Science Laboratory (MSL) rover Datasets* (Hundman et al. 2018), *Server Machine Dataset (SMD)* (Su et al. 2019) and *Secure Water Treatment (SWaT) Dataset* (Goh et al. 2016). Detailed description of datasets is listed in the appendix.

Following previous researches (Audibert et al. 2020; Su et al. 2019), we use F1 score (F1) to evaluate the performance of anomaly detection, with Precision (P) and Recall (R) for reference. In the practical situation, the importance

of precision and recall is varied according to different practical applications. For example, people often require higher recall to avoid missing fraud events in fraud detection while the requirement for precision is higher than recall in the field of operation and maintenance. Thus, we mainly use the F1 score to evaluate the performance to remove the preference of precision and recall. Besides, in order to remove the influence of threshold selection, we use brute force searching to get the best F1 score. Precision and Recall are calculated using the threshold of the best F1 score. Finally, in real-world applications, the point-wise metrics are not necessary for human operators. Alerting for any point in a contiguous anomaly segment is acceptable if the delay is not out of tolerance. We follow the settings of the modified F1 score which is widely accepted in literature (Audibert et al. 2020; Su et al. 2019). In detail, for an anomaly segment, as long as a certain point in the abnormal segment is detected by the anomaly detection method, the whole segment is considered to be abnormal.

Finally, all experiments are conducted at a node in a Xeon cluster with 32GB dedicated memory, 4 CPU cores and 1 Tesla K80 or Geforce GTX 2080 GPU accelerator.

Comparison with SOTAs

This section examines the effectiveness of MemAAE on real-life anomaly detection datasets with state-of-the-art competing methods.

Setup. We compare our proposed model with six state-of-the-art unsupervised anomaly detection methods, including Isolation Forests (IF) (Liu, Ting, and Zhou 2008), Deep Autoencoding Gaussian Mixture Model (DAGMM) (Zong et al. 2018), AE, LSTM-VAE (Park, Hoshi, and Kemp 2018), OmniAnomaly (Su et al. 2019) and USAD (Audibert et al. 2020). In the experiment, Precision, Recall and adjusted F1 score are reported for each dataset.

Results & Analysis. Table 1 shows the experimental results of our approach and baselines on the four datasets. As shown in the table, MemAAE shows superior performance and achieves best F1 scores, with gains of 1%, 4%, 0.5% and 4% on MSL, SMAP, SMD and SWAT than the best baseline respectively. The experimental results demonstrate the effectiveness of our proposed method. **It is noticed that precision and recall scores are calculated using the best F1 score's threshold. Thus they only imply that, under the best F1 situation, how are the precision and recall scores.** The experimental results demonstrate our method achieves the best trade-off between precision and recall.

In detail, IF presents the lowest performance among all baselines. The limitation of IF lies in lacking the ability to model complex normal patterns since it simply assumes that anomalies are more likely to be linearly separated in the original space. MemAAE leverages deep autoencoding to detect anomalies, which enables our method to outperform IF.

DAGMM obtains relative poor results on the four datasets. Although it utilizes deep neural networks, DAGMM focuses on anomaly detection for multivariate features without temporal correlations. It fails to model temporally dependent observations thus the performance is lagging

Table 1: Performance of MemAAE and baselines.

Model	SMAP			MSL			SMD			SWaT		
	P	R	F1									
IF	0.4423	0.5105	0.4671	0.5681	0.6740	0.5984	0.5938	0.8532	0.5866	0.9620	0.7315	0.8311
DAGMM	0.6334	0.9984	0.7124	0.7562	0.9803	0.8112	0.6730	0.8450	0.7231	0.8292	0.7674	0.7971
AE	0.7216	0.9795	0.7776	0.8535	0.9748	0.8792	0.8825	0.8037	0.8280	0.9913	0.7040	0.8233
LSTM-VAE	0.7164	0.9875	0.7555	0.8599	0.9756	0.8537	0.8698	0.7879	0.8083	0.7123	0.9258	0.8051
OmniAnomaly	0.7585	0.9756	0.8054	0.9140	0.8891	0.8952	0.9809	0.9438	0.9441	0.7223	0.9832	0.8328
USAD	0.7697	0.9831	0.8186	0.8810	0.9786	0.9109	0.9314	0.9617	0.9382	0.9870	0.7402	0.8460
MemAAE	0.8111	0.9044	0.8552	0.9112	0.9298	0.9204	0.9539	0.9439	0.9489	0.9551	0.8239	0.8847

behind. In our model, the temporal information is explicitly modeled by the prediction task. As a result, MemAAE outperforms DAGMM on all the four datasets.

Rather than conventional AE, LSTM-VAE simply stacks LSTM and VAE to model the temporal correlations. However, this approach directly replaces the feed-forward network in VAE with LSTM, i.e. aggregating information from the original inputs. From the perspective of dynamic systems, it is beneficial to summarize information from latent stochastic variables, e.g. latent vectors (Su et al. 2019). This explains the worse performance of LSTM-VAE w.r.t models using stochastic recurrent networks such as OmniAnomaly.

OmniAnomaly models temporal correlations by stochastic recurrent networks plus a normalizing flow module to deal with complex latent distributions. However, compared with MemAAE, it is still lagged behind. The main drawback of OmniAnomaly are two-fold. First, the use of VAE tends to produce over-smoothed reconstructions, which ignores slight perturbations of anomalies. Second, OmniAnomaly only uses reconstruction errors to detect anomalies, which may neglects local and contextual anomalies. As a result, MemAAE still outperforms it on all datasets.

USAD incorporates the autoencoder with adversarial training. Compared with OmniAnomaly and other reconstruction-based approaches, USAD uses an additional discriminator to amplify “mild” anomalies, which can be more sensitive for slight anomalies. However, MemAAE still exceeds USAD on all datasets. The main difficulty of USAD is that it suffers the burden of training two contending discriminators. As demonstrated in prior works (Arjovsky, Chintala, and Bottou 2017), GAN is notoriously hard to be trained. USAD may sometimes converge to a sub-optimal equilibrium, which can heavily hurt the performance.

Sensitivities w.r.t. Hyperparameters

Setup. In this section, we study the effects of different hyperparameters to the performance of MemAAE, including the reconstruction weight, the prediction weights, the size of the memory module, and the number of prediction steps. We adjust the setting of each parameter respectively and report the performance for all the four datasets.

Table 2: Quantitative results of different prediction steps.

Pred Step	SMAP			MSL			SMD			SWaT		
	P	R	F1									
5	0.977	0.552	0.705	0.842	0.795	0.818	0.878	0.921	0.899	0.557	0.733	0.633
10	0.955	0.562	0.707	0.820	0.924	0.869	0.955	0.885	0.919	0.952	0.715	0.817
15	0.789	0.722	0.754	0.809	0.786	0.797	0.929	0.931	0.930	0.585	0.715	0.643
20	0.933	0.564	0.703	0.825	0.781	0.802	0.934	0.919	0.926	0.993	0.707	0.826

Table 3: Quantitative results of different memory sizes.

Mem Size	SMAP			MSL			SMD			SWaT		
	P	R	F1									
128	0.977	0.550	0.703	0.935	0.880	0.906	0.935	0.918	0.926	0.740	0.754	0.747
256	0.972	0.552	0.704	0.774	0.883	0.825	0.934	0.906	0.920	0.878	0.723	0.793
512	0.982	0.549	0.704	0.884	0.869	0.872	0.878	0.921	0.899	0.940	0.706	0.806
1024	0.943	0.560	0.703	0.939	0.801	0.865	0.942	0.920	0.931	0.427	0.732	0.540

Reconstruction Weight λ . Firstly, we study the parameter of reconstruction weight. A larger reconstruction weight indicates more attention to the reconstruction loss contained in the overall objective. Figure 3a shows the experimental results of different reconstruction weights, in which range from [1.0, 1.5, 2.0, 2.5, 3.0]. From the experimental results, we can find that on SMAP and SMD, the performance of MemAAE is relatively stable w.r.t. reconstruction weights. Besides, the change of reconstruction weights causes large fluctuations to the performance of MemAAE on MSL and SWaT, indicating that the reconstruction loss plays a crucial role in the determination of anomalies on MSL and SWaT.

Prediction Weights γ_1 and γ_2 . We investigate the influence of two prediction weights γ_1 and γ_2 . As described above, the prediction task is designed to detect local anomalies. Since the significance of local anomalies is varied over different datasets, the choice of the prediction weight is of great importance. To study the influence of them, we use candidate settings of [1.0, 1.3, 1.5, 1.7, 2.0] and

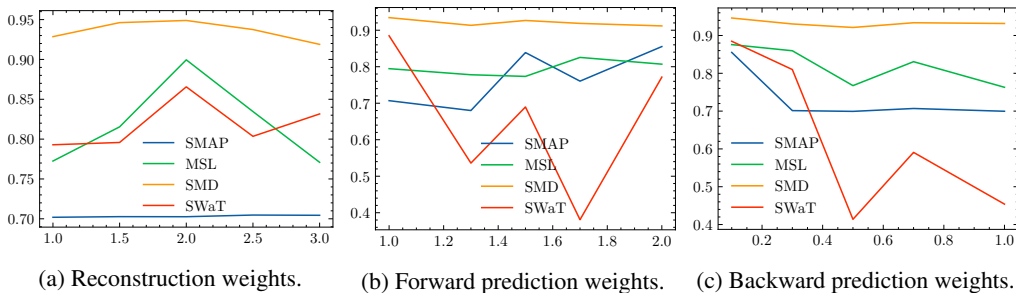


Figure 3: Sensitivity test for reconstruction weight λ , forward prediction weight γ_1 and backward prediction weight γ_2 respectively.

[0.1, 0.3, 0.5, 0.7, 1.0] for the forward prediction weight and the backward prediction weight respectively. The experimental results of the two parameters are shown in Figure 3b and Figure 3c separately. We can investigate that MSL and SMD are relatively stable for different parameter settings. Besides, SMAP and SWaT are extremely sensitive for the prediction weight. According to the experiments, we choose the settings of prediction weights empirically.

Prediction Steps T . Here we study the influence of the number of prediction steps. The prediction module performs a bi-directional forecasting to detect anomalies, especially local anomalies. As shown in Table 2, extending the range of forecasting can enlarge the receptive field of the predictor but it can not always bring a performance boost. We can investigate that the best setting of prediction steps largely depends on the specific dataset.

Memory Size M . Lastly, we study the influence of the memory size. The memory module preserves normal patterns to suppress the generalization capabilities of the autoencoder. By reconstructing samples only from the memory module, anomalies are less likely to be well reconstructed. As illustrated in Table 3, the choice of the memory size is important. Simply enlarging the scale of the memory can obtain insignificant gains (SMAP), even a performance drop (SWaT). The experimental results suggest us to select a proper value for the memory size.

Ablation Study

Setup. In this section, we examine the effectiveness of our proposed two modules: the prediction module and the memory module. In the experiment, we compare our model with its simplified counterparts, denoted as *w/o prediction* and *w/o memory*, respectively.

Table 4: Quantitative results of MemAAE and its variants.

Model	SMAP			MSL			SMD			SWaT		
	P	R	F1									
<i>w/o prediction</i>	0.939	0.566	0.706	0.844	0.725	0.780	0.918	0.945	0.931	0.974	0.719	0.827
<i>w/o memory</i>	0.974	0.548	0.702	0.846	0.830	0.838	0.922	0.909	0.915	0.972	0.731	0.834
MemAAE	0.811	0.904	0.855	0.911	0.930	0.920	0.954	0.944	0.949	0.955	0.824	0.885

Results & Analysis. As illustrated in Table 4, the memory module and the prediction module all have major contributions to the superior performance of MemAAE. Removing any of them results in degrading the original performance of the model significantly.

The memory module enables MemAAE to reduce false negatives, i.e. well-reconstructed anomalies in the evaluation phase. Without the memory module, the model can “generalize” so well such that it also reconstruct anomalies well, which will degenerate the performance. Besides, the anomalies can also appeared in the training dataset (termed *Anomaly Contamination*), since we follow a fully unsupervised setting. In this situation, the encoded latent space can be polluted by anomalous patterns without using the memory module. Thus, the memory module plays a vital role to avoid this issue.

The prediction module provides a complementary anomaly scoring approach for reconstruction errors. Generally, the reconstruction task is good at detecting global anomalies, but it may ignore local perturbations or contextual deviations, especially when the values still conform to normal range. With the help of the prediction task, this situation can be tackled since these incident deviations can hardly be predicted. By incorporating the reconstruction task, MemAAE can detect a wide range of anomalies, leading robust and effective anomaly detection in real-world applications.

Conclusion

In this paper, we propose a novel unsupervised algorithm, MemAAE, for multi-variate time series anomaly detection. Main novelties of this work are three-fold. First, by taking the advantage of adversarial training, MemAAE is able to reconstruct complex normal patterns of time-series. Second, the memory module encodes the normality manifold into memory vectors. By composing vectors drawn from the memory module, reconstructions are only computed from normal patterns. Finally, the prediction branch plays a complementary role for the reconstruction branch since forecasting future can be sensitive for local anomalies, which are hard to be captured by the reconstruction task. Extensive experiments with real-world datasets show the effectiveness and robustness of our proposed method compared with competing baselines.

References

- Aggarwal, C. C. 2016. *Outlier Analysis*. Springer Publishing Company, Incorporated, 2nd edition. ISBN 3319475770.
- Arjovsky, M.; Chintala, S.; and Bottou, L. 2017. Wasserstein Generative Adversarial Networks. In Precup, D.; and Teh, Y. W., eds., *Proceedings of the 34th International Conference on Machine Learning, ICML 2017, Sydney, NSW, Australia, 6-11 August 2017*, volume 70 of *Proceedings of Machine Learning Research*, 214–223. PMLR.
- Audibert, J.; Michiardi, P.; Guyard, F.; Marti, S.; and Zuluaga, M. A. 2020. USAD: UnSupervised Anomaly Detection on Multivariate Time Series. In *Proceedings of the 26th ACM SIGKDD International Conference on Knowledge Discovery & Data Mining*, 3395–3404.
- Braei, M.; and Wagner, S. 2020. Anomaly detection in univariate time-series: A survey on the state-of-the-art. *arXiv preprint arXiv:2004.00433*.
- Breunig, M. M.; Kriegel, H.-P.; Ng, R. T.; and Sander, J. 2000. LOF: Identifying Density-based Local Outliers. In *Proceedings of the 2000 ACM SIGMOD International Conference on Management of Data*, volume 29, 93–104. ACM.
- Chalapathy, R.; and Chawla, S. 2019. Deep Learning for Anomaly Detection: A Survey. *arXiv:1901.03407*.
- Chandola, V.; Banerjee, A.; and Kumar, V. 2009. Anomaly detection: A survey. *ACM computing surveys (CSUR)*, 41(3): 1–58.
- Chaovalitwongse, W. A.; Fan, Y.-J.; and Sachdeo, R. C. 2007. On the time series k -nearest neighbor classification of abnormal brain activity. *IEEE Transactions on Systems, Man, and Cybernetics-Part A: Systems and Humans*, 37(6): 1005–1016.
- Chung, J.; Gulcehre, C.; Cho, K.; and Bengio, Y. 2014. Empirical evaluation of gated recurrent neural networks on sequence modeling. *arXiv preprint arXiv:1412.3555*.
- Filonov, P.; Lavrentyev, A.; and Vorontsov, A. 2016. Multivariate Industrial Time Series with Cyber-Attack Simulation: Fault Detection Using an LSTM-based Predictive Data Model. *arXiv:1612.06676*.
- Georgescu, M.-I.; Barbalau, A.; Ionescu, R. T.; Khan, F. S.; Popescu, M.; and Shah, M. 2021. Anomaly detection in video via self-supervised and multi-task learning. In *Proceedings of the IEEE/CVF Conference on Computer Vision and Pattern Recognition*, 12742–12752.
- Goh, J.; Adepu, S.; Junejo, K. N.; and Mathur, A. 2016. A dataset to support research in the design of secure water treatment systems. In *International conference on critical information infrastructures security*, 88–99. Springer.
- Gong, D.; Liu, L.; Le, V.; Saha, B.; Mansour, M. R.; Venkatesh, S.; and Hengel, A. v. d. 2019. Memorizing normality to detect anomaly: Memory-augmented deep autoencoder for unsupervised anomaly detection. In *Proceedings of the IEEE/CVF International Conference on Computer Vision*, 1705–1714.
- Goodfellow, I.; Pouget-Abadie, J.; Mirza, M.; Xu, B.; Warde-Farley, D.; Ozair, S.; Courville, A.; and Bengio, Y. 2014. Generative adversarial nets. In *Advances in neural information processing systems*, 2672–2680.
- Gupta, M.; Gao, J.; Aggarwal, C. C.; and Han, J. 2013. Outlier detection for temporal data: A survey. *IEEE Transactions on Knowledge and data Engineering*, 26(9): 2250–2267.
- He, K.; Fan, H.; Wu, Y.; Xie, S.; and Girshick, R. 2020. Momentum contrast for unsupervised visual representation learning. In *Proceedings of the IEEE/CVF Conference on Computer Vision and Pattern Recognition*, 9729–9738.
- Hochreiter, S.; and Schmidhuber, J. 1997. Long short-term memory. *Neural computation*, 9(8): 1735–1780.
- Hundman, K.; Constantinou, V.; Laporte, C.; Colwell, I.; and Soderstrom, T. 2018. Detecting spacecraft anomalies using lstms and nonparametric dynamic thresholding. In *Proceedings of the 24th ACM SIGKDD international conference on knowledge discovery & data mining*, 387–395.
- Kieu, T.; Yang, B.; Guo, C.; and Jensen, C. S. 2019. Outlier Detection for Time Series with Recurrent Autoencoder Ensembles. In *Proceedings of the Twenty-Eighth International Joint Conference on Artificial Intelligence, IJCAI-19*, 2725–2732. International Joint Conferences on Artificial Intelligence Organization.
- Kingma, D. P.; and Ba, J. 2015. Adam: A Method for Stochastic Optimization. In Bengio, Y.; and LeCun, Y., eds., *3rd International Conference on Learning Representations, ICLR 2015, San Diego, CA, USA, May 7-9, 2015, Conference Track Proceedings*.
- Kingma, D. P.; and Welling, M. 2014. Auto-Encoding Variational Bayes. In Bengio, Y.; and LeCun, Y., eds., *2nd International Conference on Learning Representations, ICLR 2014, Banff, AB, Canada, April 14-16, 2014, Conference Track Proceedings*.
- Laptev, N.; Amizadeh, S.; and Flint, I. 2015. Generic and scalable framework for automated time-series anomaly detection. In *Proceedings of the 21th ACM SIGKDD international conference on knowledge discovery and data mining*, 1939–1947.
- Li, D.; Chen, D.; Jin, B.; Shi, L.; Goh, J.; and Ng, S.-K. 2019. Mad-gan: Multivariate anomaly detection for time series data with generative adversarial networks. In *International Conference on Artificial Neural Networks*, 703–716. Springer.
- Li, L.; Yan, J.; Wang, H.; and Jin, Y. 2021. Anomaly Detection of Time Series With Smoothness-Inducing Sequential Variational Auto-Encoder. *IEEE Transactions on Neural Networks and Learning Systems*, 32(3): 1177–1191.
- Li, Z.; Chen, W.; and Pei, D. 2018. Robust and Unsupervised KPI Anomaly Detection Based on Conditional Variational Autoencoder. In *37th IEEE International Performance Computing and Communications Conference, IPCCC 2018, Orlando, FL, USA, November 17-19, 2018*, 1–9.
- Li, Z.; Zhao, Y.; Botta, N.; Ionescu, C.; and Hu, X. 2020. COPOD: copula-based outlier detection. *arXiv preprint arXiv:2009.09463*.
- Liu, D.; Zhao, Y.; Xu, H.; Sun, Y.; Pei, D.; Luo, J.; Jing, X.; and Feng, M. 2015. Opprentice: Towards Practical and Automatic Anomaly Detection Through Machine Learning. In

- Proceedings of the 2015 Internet Measurement Conference, IMC '15*, 211–224. New York, NY, USA: Association for Computing Machinery. ISBN 9781450338486.
- Liu, F. T.; Ting, K. M.; and Zhou, Z.-H. 2008. Isolation forest. In *2008 eighth IEEE international conference on data mining*, 413–422. IEEE.
- Ma, J.; and Perkins, S. 2003. Time-series novelty detection using one-class support vector machines. In *Proceedings of the International Joint Conference on Neural Networks, 2003.*, volume 3, 1741–1745. IEEE.
- Makhzani, A.; Shlens, J.; Jaitly, N.; Goodfellow, I.; and Frey, B. 2015. Adversarial autoencoders. *arXiv preprint arXiv:1511.05644*.
- Malhotra, P.; Ramakrishnan, A.; Anand, G.; Vig, L.; Agarwal, P.; and Shroff, G. 2016. LSTM-based Encoder-Decoder for Multi-sensor Anomaly Detection. *arXiv:1607.00148*.
- Pang, G.; Shen, C.; Cao, L.; and Hengel, A. V. D. 2021. Deep Learning for Anomaly Detection: A Review. *ACM Computing Surveys (CSUR)*, 54(2): 1–38.
- Park, D.; Hoshi, Y.; and Kemp, C. C. 2018. A multimodal anomaly detector for robot-assisted feeding using an lstm-based variational autoencoder. *IEEE Robotics and Automation Letters*, 3(3): 1544–1551.
- Park, H.; Noh, J.; and Ham, B. 2020. Learning memory-guided normality for anomaly detection. In *Proceedings of the IEEE/CVF Conference on Computer Vision and Pattern Recognition*, 14372–14381.
- Ramaswamy, S.; Rastogi, R.; and Shim, K. 2000. Efficient algorithms for mining outliers from large data sets. In *Proceedings of the 2000 ACM SIGMOD international conference on Management of data*, 427–438.
- Rumelhart, D. E.; Hinton, G. E.; and Williams, R. J. 1985. Learning internal representations by error propagation. Technical report, California Univ San Diego La Jolla Inst for Cognitive Science.
- Sadhu, V.; Misu, T.; and Pompili, D. 2019. Deep multi-task learning for anomalous driving detection using CAN bus scalar sensor data. In *2019 IEEE/RSJ International Conference on Intelligent Robots and Systems (IROS)*, 2038–2043. IEEE.
- Schuster, M.; and Paliwal, K. 1997. Bidirectional recurrent neural networks. *IEEE Transactions on Signal Processing*, 45(11): 2673–2681.
- Siffer, A.; Fouque, P.; Termier, A.; and Largouët, C. 2017. Anomaly Detection in Streams with Extreme Value Theory. In *Proceedings of the 23rd ACM SIGKDD International Conference on Knowledge Discovery and Data Mining, Halifax, NS, Canada, August 13 - 17, 2017*, 1067–1075. ACM.
- Su, Y.; Zhao, Y.; Niu, C.; Liu, R.; Sun, W.; and Pei, D. 2019. Robust Anomaly Detection for Multivariate Time Series through Stochastic Recurrent Neural Network. In *Proceedings of the 25th ACM SIGKDD International Conference on Knowledge Discovery & Data Mining*, 2828–2837.
- Tian, H.; Khoa, N. L. D.; Anaissi, A.; Wang, Y.; and Chen, F. 2019. Concept Drift Adaption for Online Anomaly Detection in Structural Health Monitoring. In *Proceedings of the 28th ACM International Conference on Information and Knowledge Management, CIKM '19*, 2813–2821. New York, NY, USA: Association for Computing Machinery. ISBN 9781450369763.
- Wu, Z.; Xiong, Y.; Yu, S. X.; and Lin, D. 2018. Unsupervised feature learning via non-parametric instance discrimination. In *Proceedings of the IEEE conference on computer vision and pattern recognition*, 3733–3742.
- Xu, H.; Chen, W.; Zhao, N.; Li, Z.; Bu, J.; Li, Z.; Liu, Y.; Zhao, Y.; Pei, D.; Feng, Y.; et al. 2018. Unsupervised Anomaly Detection via Variational Auto-encoder for Seasonal KPIs in Web Applications. In *Proceedings of the 2018 World Wide Web Conference*, 187–196. International World Wide Web Conferences Steering Committee.
- Zenati, H.; Romain, M.; Foo, C.-S.; Lecouat, B.; and Chandrasekhar, V. 2018. Adversarially Learned Anomaly Detection. *2018 IEEE International Conference on Data Mining (ICDM)*, 727–736.
- Zhang, Y.; and Yang, Q. 2021. A survey on multi-task learning. *IEEE Transactions on Knowledge and Data Engineering*.
- Zhao, Y.; Deng, B.; Shen, C.; Liu, Y.; Lu, H.; and Hua, X.-S. 2017. Spatio-temporal autoencoder for video anomaly detection. In *Proceedings of the 25th ACM international conference on Multimedia*, 1933–1941.
- Zhou, B.; Liu, S.; Hooi, B.; Cheng, X.; and Ye, J. 2019. BeatGAN: anomalous rhythm detection using adversarially generated time series. In *Proceedings of the 28th International Joint Conference on Artificial Intelligence*, 4433–4439. AAAI Press.
- Zong, B.; Song, Q.; Min, M. R.; Cheng, W.; Lumezanu, C.; Cho, D.; and Chen, H. 2018. Deep Autoencoding Gaussian Mixture Model for Unsupervised Anomaly Detection. In *International Conference on Learning Representations*.

Appendix

Data Preprocessing

Data normalization. We rescale the time-series into the range $[0, 1]$ using minimum values and maximum values of the training data:

$$\tilde{x} = \frac{x - \min(X_{\text{train}})}{\max(X_{\text{train}}) - \min(X_{\text{train}})}, \quad (15)$$

where $\max(X_{\text{train}})$ and $\min(X_{\text{train}})$ denote the maximum value and the minimum value of training data respectively.

Sliding window. Instead of feeding observations at each timestamp to the model, we consider the observation and its context predecessors. Thus, we apply sliding window with a length $W \ll N$ over the time-series and get the reformed dataset $\mathbf{X} \in \mathbb{R}^{(N-W+1) \times W \times K}$ where each window $\mathbf{x} \in \mathbb{R}^{W \times K}$ is the basic element.

Implementation Details

In terms of network architectures, we implement the autoencoder via one dimensional convolutional networks (1D ConvNet). We choose convolutional networks rather than fully connected networks, e.g. (Xu et al. 2018; Su et al. 2019; Audibert et al. 2020), because they are more computationally effective for large datasets. The discriminator shares the same architecture with the encoder, but outputs a single real value. The prediction module is composed of bi-directional LSTM (Schuster and Paliwal 1997), with 2 stacked fully-connected layer for each recurrent cell. We use Adam (Kingma and Ba 2015) to perform the gradient descent with a learning rate of 10^{-3} . To guarantee a comprehensive optimization, we train our model using 150 epochs with 512 mini-batches in each epoch. Other quantitative settings of hyperparameters are described in Table 5.

Dataset Details

The details of datasets are described as following:

- *Soil Moisture Active Passive (SMAP) satellite and Mars Science Laboratory (MSL) rover Datasets*¹. SMAP and MSL are released by NASA (Hundman et al. 2018) with annotations collected from real-world. They contain the data of 55 and 27 entities with 25 and 55 metrics for each respectively.
- *Server Machine Dataset (SMD)*². SMD (Su et al. 2019) is publicly released by a large Internet company and the data is monitored by 38 variables with time spanning of 5 weeks. It is divided into two subsets with equal size: one for training and the other for testing.
- *Secure Water Treatment (SWaT) Dataset*³. SWaT (Goh et al. 2016) is a scaled down version produced by a real-world industrial water treatment plant to understand the

conditions under cyber attacks. It is systematically generated from the testbed with 11 days of continuous operation: 7 days under normal operation and 4 days with attack scenarios from all the 51 sensors and actuators.

Table 5: Statistics and parameter settings of each dataset.

	SMAP	MSL	SMD	SWaT
Train	135,183	58,317	708,405	496,800
Test	427,617	73,729	708,420	449,919
Dimensions	55×25	27×55	28×38	51
Anomaly ratio (%)	13.13	10.72	4.16	11.98
Window size	32	32	32	32
Latent size	16	16	16	16
Memory size	512	512	512	512
Pred step	7	7	30	5
Reconstruction weight	1.0	1.0	2.0	1.1
Forward prediction weight	2.0	1.4	0.2	1.0
Backward prediction weight	0.1	0.2	0.1	0.1

¹<https://github.com/khundman/telemanom>

²<https://github.com/NetManAI/Ops/OmniAnomaly>

³[https://itrust.sutd.edu.sg/testbeds/secure-water-treatment-](https://itrust.sutd.edu.sg/testbeds/secure-water-treatment-swat/)